CFO impact analysis in cell free MIMO-OFDM in millimeter wave spectrum

Antony Pottier, Valerian Mannoni, Jean-Baptiste Dore

CFO Impact Analysis in Cell Free MIMO-OFDM in Millimeter Wave Spectrum

Antony Pottier, Valérian Mannoni, Jean-Baptiste Doré
CEA-Leti, Université Grenoble Alpes, F-38000 Grenoble, France
Email: {antony.pottier, valerian.mannoni, jean-baptiste.dore@cea.fr}@cea.fr

***Abstract*—This paper presents a study of a downlink (DL) cell-free MIMO-OFDM transmission under maximal ratio transmission (MRT) and full pilot zero-forcing precoding (FZF) in the presence of carrier frequency offsets (CFO). This hardware impairment causes intercarrier interference (ICI) which degrades the transmission performance. We derive closed form expressions of the achievable spectral efficiency considering frequency selective, uncorrelated, Rayleigh fading channels. Numerical results are obtained considering a transmission scenario using 5G RedCap specifications in the millimeter wave band to illustrate our derivations and quantify the performance for different values of the CFO.**

***Index Terms*—cell free, carrier frequency offset, MIMO-OFDM, precoding, hardware impairement, capacity**

I. Introduction

Cellular networks are organized according to a centralized architecture where every user in a cell is connected to a single base station. Depending on its position within the cell, the link quality of a given user can be reduced by intercell interference which reduces the overall coverage of the network. Cell free networks are envisioned to overcome the coverage limits of traditional cellular technologies and are the topic of recent researches on fith generation (5G) and beyond networks. In a cell free network, any user equipment (UE) can be connected simultaneously to several access points (APs). Every access point (AP) is equipped with several antennas and rely on Multiple Input Multiple Output (MIMO) or massive MIMO technologies to serve coherently the user equipments (UEs).

Standard works on cell free networks [1]–[4] focused on capacity bounds for precoding and combining schemes assuming MIMO Rayleigh flat fading channels and single carrier communications. Rice fading with phase shifts of the Line of Sight (LoS) component due to small displacements of UE is investigated in [5], where the specific MMSE channel estimator and capacity bounds are derived for the problem. Hardaware impairments is analyzed in uplink (UL) transmissions considering phase noise and additive distortion from power amplifiers and ADCs. Achievable rates with MMSE combining is derived in closed form from deterministic equivalents theory. An "hardware aware" MMSE combiner is also derived and comparison is carried between separate and common local oscillator for the antennas of the AP where the latter offers the best performance. This work assumes single carrier communications in correlated Rayleigh fading channels. Only few works have addressed the same studies in a multi-carrier setting, where hardware impairments such as carrier frequency offsets (CFO) due to oscillator mismatches cause Inter-Carrier Interference (ICI). One can cite for example [6] where the effect of residual CFO on cell free massive MIMO OFDM is considered only in the UL case under Maximal Ratio Combining (MRC) in a known deterministic channel and the effects of ICI are not characterized. The similar but more complete work of [7] studies the UL of cell-free MIMO OFDM with ICI due to Doppler frequency offset (DFO) in high speed train communications and provide closed form expressions of the spectral efficiency under MRC and Minimum Mean Square Error (MMSE) combining with Large Scale Fading Decoding (LSFD) at the CPU. Several power control algorithms designed to reduce the impact of DFO are also evaluated. However, this work relies on the simplifying assumption that the channels are frequency-flat over several adjacent subcarriers which can limit the applicability of their results.

The present work ambitions to fill the lack of studies on cell-free MIMO OFDM transmission under CFO in the DL, where the channel is frequency-selective and the CFO is applied to both APs and UEs sides. We provide closed-form expressions of the spectral efficiency under Maximal Ratio Transmission (MRT) and Full pilot Zero Forcing (FZF) precoding, assuming uncorrelated Rayleigh fading channels with no further simplifying assumptions regarding the channels frequency selectivity. The effects of ICI due to CFO are fully characterized. Results illustrate the performance loss due to CFO and Monte-Carlo simulations show the validity of our theoretical derivations, where we focus on application in the millimeter wave band (around 26 GHz here) using the specifications of 5G RedCap radio interface in terms of bandwidth and subcarrier spacing [8]. From an operational point of view, it is also shown that MRT seems more robust to Carrier Frequency Offset (CFO)-induced ICI than FZF precoding.

The paper is organized as follows: the system model is presented in Section II, where we briefly review the cell-free DL transmissions in a single carrier case to introduce some notations and useful signal models before generalizing to multi-carrier transmissions with CFO. In Section III is developed the theoretical study of the spectral efficiency performance of cell-free MIMO-OFDM with CFO under FZF and MRT precoding schemes. Numerical results illustrating the rate cumulative distribution functions for a simulated indoor scenario at a 26GHz center frequency using the 5G RedCap radio interface are discussed in Section IV before conclusions

in Section V.

Notations: All signal vectors or matrices are denoted by $\boldsymbol{x}$ or $\boldsymbol{X}$ respectively. The n^{th} signal sample, vector coordinate, or the element at indexes (n, m) of a matrix are denoted x_n, $\boldsymbol{x}_n$ or $\boldsymbol{X}_{n,m}$ respectively. When explicitly expressed in the frequency domain, signals components or vectors/matrices coordinates are denoted by $x[\nu]$, $\boldsymbol{x}[\nu]$, $\boldsymbol{X}[\nu, \mu]$ which corresponds to the time domain counterparts $x(n)$, $\boldsymbol{x}(n)$, $\boldsymbol{X}(n, m)$. Distinctions between discrete or continuous time signals are made clear from the context. Finally, $\mathbb{E}[X]$ denotes the expectation of a random variable X and $\mathbb{V}[X]$ its variance.

II. System Model

A. Review of the single carrier DL case

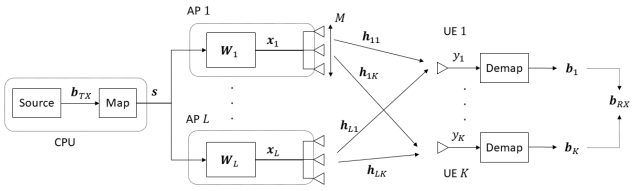

Fig. 1. Illustration of a (single carrier) cell-free MIMO transmission between L APs and K UEs.

The case of DL single carrier cell-free MIMO transmission without CFO is briefly exposed to introduce some notations, and is illustrated in Figure 1. Then, the model will be extended to MIMO-OFDM with CFO.

Following classical works on the topic [1]–[3], a cell-free MIMO system is considered assuming Time Division Duplex (TDD) transmissions between K single-antenna UEs and L APs each equipped with M antennas, serving simultaneously the UEs in the same resource blocks, and connected to a central processing unit (CPU) through a fronthaul network. In the DL, the CPU is responsible for providing symbols intended to the UEs and transmitted by the APs after local precoding. For ease of presentation, all the L APs are assumed to serve all the K UEs in the system. This is a simplification of the framework presented in [1, Section IV] where dynamic cooperation clustering is considered to link each UE to a subset of APs, according to some matrix establishing the AP-UE correspondence. The transmission is divided into coherence blocks of length $N_C = N_U + N_D$ given in number of symbols, where N_U is the length of the UL phase where the UEs send pilots and data to the APs. Conversely, N_D is the length of the DL phase where the APs serve the UEs. The precoder matrix $\boldsymbol{W}_l$ of each AP is computed on the basis of the channel estimates acquired during the UL, and assuming channel reciprocity. The UL is not discussed in anymore details in what follows[1]. The UEs are assumed to apply a simple demapping of their respective received signals to decide the received bits. The transmitted K-dimensional vector of i.i.d. zero-mean and unit variance symbols is denoted by $\boldsymbol{s}$, and is sent at the input of each AP $l \in \{1, \cdots, L\}$. The signal sent by AP l is the precoded M-dimensional vector $\boldsymbol{x}_l$ defined by

$$\boldsymbol{x}_l = \boldsymbol{W}_l \boldsymbol{s} = \sum_{k=1}^{K} \boldsymbol{w}_{lk} s_k \tag{1}$$

where $\boldsymbol{W}_l = (\boldsymbol{w}_{l1}, \cdots, \boldsymbol{w}_{lK}) \in \mathbb{C}^{M \times K}$ with the precoding vector of user $k \in \{1, \cdots, K\}$ denoted by $\boldsymbol{w}_{lk} \in \mathbb{C}^M$. A constraint on transmission power applies to each AP, which then serves UEs $k = 1 \cdots K$ with different powers. It is also assumed that $\mathbb{E}\left[\|\boldsymbol{w}_{lk}\|^2\right] = 1$.

The channels are assumed to be randomly drawn for each coherence block and fixed during the N_C symbols of one block. Denoting by $\boldsymbol{h}_{lk} \in \mathbb{C}^M$ the (UL) channel linking AP l and UE k, the signal at the receiver's input of that user is then

$$y_k = \sum_{l=1}^{L} \sqrt{p_{lk}} \boldsymbol{h}_{lk}^H \boldsymbol{w}_{lk} s_k + \sum_{j \neq k} \sum_{l=1}^{L} \sqrt{p_{lj}} \boldsymbol{h}_{lk}^H \boldsymbol{w}_{lj} s_j + n_k \tag{2}$$

where n_k is a sample of circularly symmetric gaussian noise with zero mean and variance $\sigma^2 = N_0 B$ where N_0 is the noise power spectral density and B the transmission bandwidth.

B. DL MIMO-OFDM transmission with ICI due to uncompensated CFO

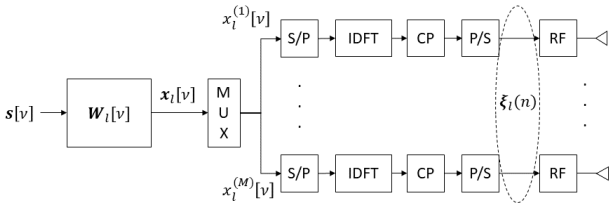

Fig. 2. MIMO-OFDM transmitter of an AP l with precoding.

Considering OFDM transmissions, the transmitter's structure of an AP l is depicted in Figure 2. Given a sampling period T, the transmission bandwidth $B = 1/T$ is divided into N subcarriers of width $\Delta_f = 1/T_s$ with $T_s = N/B$. The Orthogonal Frequency Division Multiplex (OFDM) symbol duration is $T_{\text{bl}} = T_s + T_g$ with T_g the cyclic prefix (CP) duration assumed to absorb the channel delay spread. A vector of symbols $\boldsymbol{s}[\nu] \in \mathbb{C}^K$, for the K users served and each subcarrier $\nu \in \{0, \cdots, N-1\}$, is pushed at the input of all the access points. These symbols are i.i.d, zero-mean, unit variance, and are precoded with the matrix $\boldsymbol{W}_l[\nu] = (\boldsymbol{w}_{l1}[\nu], \cdots, \boldsymbol{w}_{lK}[\nu])$, which depends on the channel estimates on the subcarrier ν for each user. Let $p_{lk}[\nu]$ be the transmitted power of AP l on subcarrier ν of UE k. A total transmit power constraint must be fulfilled, so that $\sum_\nu p_{lk}[\nu] = \bar{p}_{lk}$ and $\sum_k \bar{p}_{lk} = P_{tx}$ for each AP. In this paper we limit ourselves to uniform power allocation across the bandwidth and we let $p_{lk}[\nu] = p_{lk}$ for all ν. An OFDM modulator operates on each transmit antenna $m = 1, \cdots, M$ by an N-dimensional Inverse Discrete Fourier Transform (IDFT) and CP insertion, which is neglected in the

[1]Note that we will also not discuss pilot contamination, which can also be avoided through dynamic cooperation clustering by a proper pilot allocation among UEs, see [1]. Furthermore, the fact that we will focus on OFDM transmission could also be exploited to limit such effects, see [9]

following equations for convenience[2]. At sample time n, the M-dimensional vector at the output of the modulator l is

$$\boldsymbol{\xi}_l(n) \triangleq \frac{1}{\sqrt{N}} \sum_{\nu=0}^{N-1} \boldsymbol{x}_l[\nu] e^{\,\mathrm{j}\frac{2\pi}{N}\nu n} \tag{3}$$

where $\boldsymbol{x}_l[\nu] = \boldsymbol{W}_l[\nu]\boldsymbol{P}_l[\nu]\boldsymbol{s}[\nu]$ and $\boldsymbol{P}_l[\nu] \triangleq \mathrm{diag}(p_{lk})_{k=1}^{K}$.

At the receiver side, after CP removal and Discrete Fourier Transform (DFT) assuming first no CFO, the signal received at the ν^{th} subcarrier by UE k can be written as in (2) but for each subcarrier $\nu = 0, \cdots, N-1$. Let us suppose now that each AP l and each UE k are affected by a CFO denoted respectively by $\varphi_l = \epsilon_l f_c/\Delta_f$ and $\theta_k = \epsilon_k f_c/\Delta_f$, where f_c is the carrier frequency. Then, the N samples of an OFDM symbol sent by AP l are multiplied by $e^{\,\mathrm{j}2\pi\varphi_l n/N}$, with $n = 0, \cdots, N-1$, and conversely the signal samples received by UE k are multiplied by $e^{\,\mathrm{j}2\pi\theta_k n/N}$. Using the developments derived in Appendix A, it is straightforward to show that the received signal at UE k is expressed by

$$\begin{aligned} y_k[\nu] = &\sum_{l=1}^{L}\sum_{\mu=0}^{N-1} \sqrt{p_{lk}}\zeta_{lk}^{k}[\mu]s_k[\mu]\psi_{lk}[\nu-\mu] \\ &+ \sum_{j\neq k}\sum_{l=1}^{L}\sum_{\mu=0}^{N-1} \sqrt{p_{lj}}\zeta_{lk}^{j}[\mu]s_j[\mu]\psi_{lk}[\nu-\mu] + n_k[\nu] \end{aligned} \tag{4}$$

where $\zeta_{lk}^{j}[\nu] = \boldsymbol{h}_{lk}^{H}[\nu]\boldsymbol{w}_{lj}[\nu]$ and $\psi_{lk}[\nu] = \psi_{\varphi_l+\theta_k}[\nu]$ is defined as in equation (29) of Appendix A, setting $\varphi = \varphi_l + \theta_k$. Uncorrelated Rayleigh fading is assumed for the remaining of the paper so that every channel vector $\boldsymbol{h}_{lk}[\nu] \sim \mathcal{CN}(\boldsymbol{0}, \beta_{lk}\boldsymbol{I}_M)$ with the same pathloss for all subcarriers $\nu = 0, \cdots, N-1$. The noise n_k is circularly symmetric complex gaussian with zero-mean and variance $\sigma^2 = N_0\Delta_f$.

C. UL transmission and channel estimation

During the UL phase the UEs send their pilot symbols synchronously to the APs, prior to data transmission. The ICI and the effects of CFO are neglected during the UL pilot transmission and channel estimation phase. Pilot contamination can be avoided considering that pilots can be transmitted using orthogonal patterns over several OFDM symbols, or that each user is allocated one OFDM symbol in a frame to transmit its pilots, while the others remain silent (see for example [9]). Focusing on subcarrier ν, and assuming that the UE k sends a known pilot symbol $q_k[\nu]$ such that $|q_k[\nu]|^2 = 1$, the MMSE channel estimation on that subcarrier can easily be determined through standard computations from estimation theory [11] applied to the following observation

$$\boldsymbol{y}_l[\nu] = \boldsymbol{h}_{lk}[\nu] + \boldsymbol{n}_l[\nu] \tag{5}$$

where $\boldsymbol{n}_l[\nu] \sim \mathcal{CN}(\boldsymbol{0}, \sigma^2\boldsymbol{I}_M)$. The MMSE estimate of $\boldsymbol{h}_{lk}[\nu]$ is given by

$$\hat{\boldsymbol{h}}_{lk}[\nu] = \frac{\beta_{lk}}{\beta_{lk}+\sigma^2}\boldsymbol{y}_l[\nu]. \tag{6}$$

[2]Incorporating the cyclic prefix explicitly in the signals models requires to define two extra matrices for CP insertion and removal respectively, see for example [10]

We then have $\hat{\boldsymbol{h}}_{lk}[\nu] \sim \mathcal{CN}(\boldsymbol{0}, \gamma_{lk}\boldsymbol{I}_M)$ where $\gamma_{lk} = \frac{\beta_{lk}^2}{\beta_{lk}+\sigma^2}$, and the estimation error $\tilde{\boldsymbol{h}}_{lk}[\nu] = \boldsymbol{h}_{lk}[\nu] - \hat{\boldsymbol{h}}_{lk}[\nu] \sim \mathcal{CN}(\boldsymbol{0}, (\beta_{lk}-\gamma_{lk})\boldsymbol{I}_M)$.

III. Performance of the DL with CFO

In what follows, the spectral efficiency (SE) of DL cell-free MIMO-OFDM transmissions in the presence of ICI is derived in the general case, based on the *use and then forget* (UatF) lower bound on the capacity of deterministic channels polluted by additive white gaussian noise and uncorrelated interference [12]. Expressions for the SE of MRT and FZF precoders are then derived considering the transmissions take place in Rayleigh fading channels.

A. DL SINR and spectral efficiency

The received signal in (4) may be decomposed into the sum of five components : coherent precoding (CP), precoder uncertainty (PU), ICI, multiuser interference (UI) and noise. We thus have

$$\begin{aligned} y_k[\nu] = &\, CP_k[\nu]s_k[\nu] + PU_k[\nu]s_k[\nu] \\ &+ \sum_{\mu\neq\nu} ICI_k[\nu-\mu]s_k[\mu] \\ &+ \sum_{j\neq k}\sum_{\mu=0}^{N-1} UI_{jk}[\nu-\mu]s_j[\mu] + n_k[\nu] \end{aligned} \tag{7}$$

with

$$CP_k[\nu] = \sum_{l=1}^{L} \sqrt{p_{lk}}\psi_{lk}[0]\mathbb{E}\left[\zeta_{lk}^{k}[\nu]\right] \tag{8}$$

$$PU_k[\nu] = \sum_{l=1}^{L} \sqrt{p_{lk}}\psi_{lk}[0](\zeta_{lk}^{k}[\nu] - \mathbb{E}\left[\zeta_{lk}^{k}[\nu]\right]) \tag{9}$$

$$ICI_k[\nu-\mu] = \sum_{l=1}^{L} \sqrt{p_{lk}}\zeta_{lk}^{k}[\mu]\psi_{lk}[\nu-\mu] \tag{10}$$

$$UI_{jk}[\nu-\mu] = \sum_{l=1}^{L} \sqrt{p_{lj}}\zeta_{lk}^{j}[\mu]\psi_{lk}[\nu-\mu], \tag{11}$$

Proposition 1. *The theoretical channel capacity of user k is lower bounded by*

$$SE_k = \sum_{\nu=0}^{N-1} \log_2\left(1 + SINR_k[\nu]\right) \tag{12}$$

in bits/s/Hz with the DL SINR of UE k given in (13)*.*

This statement follows directly from [12, Corollary 1.3, p.171], since it can easily be checked that, for each subcarrier ν, every interference term expressed in (7) is uncorrelated with the useful part of the signal given by $CP_k[\nu]s_k[\nu]$.

B. Maximal Ratio Transmission in Rayleigh fading

The MRT precoding vector of AP l towards UE k is given, for each subcarrier ν, by

$$\boldsymbol{w}_{lk}^{\mathrm{mrt}}[\nu] \triangleq \frac{\hat{\boldsymbol{h}}_{lk}[\nu]}{\sqrt{\mathbb{E}\left[\left\|\hat{\boldsymbol{h}}_{lk}[\nu]\right\|^2\right]}} = \frac{\hat{\boldsymbol{h}}_{lk}[\nu]}{\sqrt{M\gamma_{lk}}}. \tag{15}$$

$$SINR_k[\nu] = \frac{|CP_k[\nu]|^2}{\sigma^2 + \mathbb{E}\left[|PU_k[\nu]|^2\right] + \sum_{\mu\neq\nu}\mathbb{E}\left[|ICI_k[\nu-\mu]|^2\right] + \sum_{j\neq k}\sum_{\mu=0}^{N-1}\mathbb{E}\left[|UI_{jk}[\nu-\mu]\right]|^2} r \tag{13}$$

$$= \frac{\left|\sum_{l=1}^{L}\sqrt{p_{lk}}\psi_{lk}[0]\mathbb{E}\left[\zeta_{lk}^{k}[\nu]\right]\right|^2}{\sigma^2 + \sum_{j=1}^{K}\sum_{\mu=0}^{N-1}\mathbb{E}\left[\left|\sum_{l=1}^{L}\sqrt{p_{lj}}\psi_{lk}[\nu-\mu]\zeta_{lk}^{j}[\mu]\right|^2\right] - \left|\sum_{l=1}^{L}\sqrt{p_{lk}}\psi_{lk}[0]\mathbb{E}\left[\zeta_{lk}^{k}[\nu]\right]\right|^2} \tag{14}$$

We define the following terms

$$\zeta_{lk}^{k}[\nu] \triangleq \frac{\boldsymbol{h}_{lk}^{H}[\nu]\hat{\boldsymbol{h}}_{lk}[\nu]}{\sqrt{M\gamma_{lk}}} \quad \text{and} \quad \zeta_{lk}^{j}[\nu] \triangleq \frac{\boldsymbol{h}_{lk}[\nu]^{H}\hat{\boldsymbol{h}}_{lj}[\nu]}{\sqrt{M\gamma_{lj}}}$$

Thus, using that $\boldsymbol{h}_{lk}[\nu] = \hat{\boldsymbol{h}}_{lk}[\nu] + \tilde{\boldsymbol{h}}_{lk}[\nu]$ is zero-mean and decorrelated from $\hat{\boldsymbol{h}}_{lk}[\nu]$ and $\boldsymbol{h}_{lj}[\nu]$ if $j \neq k$, we have

$$\mathbb{E}\left[\zeta_{lk}^{j}[\nu]\right] = \begin{cases} \sqrt{M\gamma_{lk}} & j = k \\ 0 & j \neq k \end{cases} \tag{16}$$

and noticing that $\hat{\boldsymbol{h}}_{lk}^{H}\hat{\boldsymbol{h}}_{lk}/\sqrt{M\gamma_{lk}}$ is a χ^2_M random variable with mean $\sqrt{M\gamma_{lk}}$ and variance γ_{lk}, straightforward algebra shows that

$$\mathbb{E}\left[\left|\zeta_{lk}^{j}[\nu]\right|^2\right] = \begin{cases} M\gamma_{lk} + \beta_{lk} & j = k \\ \beta_{lk} & j \neq k \end{cases} \tag{17}$$

Furthermore, since $\left(\zeta_{lk}^{j}\right)_{l=1}^{L}$ is a sequence of independent random variables, we have

$$\mathbb{E}\left[\left|\sum_{l=1}^{L} a_{ljk}\zeta_{lk}^{j}[\mu]\right|^2\right] = \sum_{l=1}^{L}|a_{ljk}|^2\,\mathbb{V}\left[\zeta_{lk}^{j}[\mu]\right] + \left|\sum_{l=1}^{L} a_{ljk}\mathbb{E}\left[\zeta_{lk}^{j}[\mu]\right]\right|^2 \tag{18}$$

where $a_{ljk} \triangleq \sqrt{p_{lj}}\psi_{lk}[\nu-\mu]$, and using (16) and (17), it can easily be shown that $\forall j$

$$\mathbb{V}\left[\zeta_{lk}^{j}[\mu]\right] = \beta_{lk} \tag{19}$$

Plugging (16)-(19) to the SINR expressed in (14) yields the SINR on the ν^{th} subcarrier of user k under MRT precoding in the presence of ICI given by (20). The interference term under MRT is splitted into two disctinct terms: the first one is the ICI depending on the coherent precoding gain on adjacent subcarriers, while the second term aggregates both the precoding uncertainties of all users, the multiuser interference and ICI from other users. The theoreteical spectral efficiency then follows from Proposition 1.

C. Full-pilot Zero Forcing in Rayleigh fading

Using the full-pilot FZF precoding scheme, the precoder vector of UE k computed by AP l is

$$\boldsymbol{w}_{lk}^{\text{zf}}[\nu] = \frac{\hat{\boldsymbol{H}}_l[\nu]\left(\hat{\boldsymbol{H}}_l^{H}[\nu]\hat{\boldsymbol{H}}_l[\nu]\right)^{-1}\boldsymbol{e}_k}{\sqrt{\mathbb{E}\left[\left\|\hat{\boldsymbol{H}}_l[\nu]\left(\hat{\boldsymbol{H}}_l^{H}[\nu]\hat{\boldsymbol{H}}_l[\nu]\right)^{-1}\boldsymbol{e}_k\right\|^2\right]}} = \sqrt{\gamma_{lk}(M-K)}\hat{\boldsymbol{H}}_l[\nu]\left(\hat{\boldsymbol{H}}_l^{H}[\nu]\hat{\boldsymbol{H}}_l[\nu]\right)^{-1}\boldsymbol{e}_k \tag{21}$$

where $\hat{\boldsymbol{H}}_l[\nu] = \left(\hat{\boldsymbol{h}}_{l1}[\nu], \cdots, \hat{\boldsymbol{h}}_{lK}[\nu]\right)$ and the normalization factor in (21) comes from standard results for inverse Wishart matrices. Let $\alpha_{lk}^{j}[\nu] = \hat{\boldsymbol{h}}_{lk}^{H}[\nu]\boldsymbol{w}_{lj}[\nu]$, so that $\zeta_{lk}^{j}[\nu] = \alpha_{lk}^{j}[\nu] + \tilde{\boldsymbol{h}}_{lk}^{H}[\nu]\boldsymbol{w}_{lj}[\nu]$. We have

$$\mathbb{E}\left[\zeta_{lk}^{j}[\nu]\right] = \alpha_{lk}^{j}[\nu] = \begin{cases} \sqrt{\gamma_{lk}(M-K)} & j = k \\ 0 & j \neq k \end{cases} \tag{22}$$

From (14) and (18), we only need the ICI terms $\psi_{lk}[\nu-\mu]$, the average precoded channel $\mathbb{E}\left[\zeta_{lk}^{j}\right]$ and its variance $\mathbb{V}\left[\zeta_{lk}^{j}\right]$ to compute the SINR of user k on any given subcarrier ν. It remains to determine $\mathbb{V}\left[\zeta_{lk}^{j}\right]$ in the FZF case :

$$\mathbb{V}\left[\zeta_{lk}^{j}\right] = \mathbb{V}\left[\alpha_{lk}^{j} + \tilde{\boldsymbol{h}}_{lk}^{H}\boldsymbol{w}_{lj}\right] = \mathbb{V}\left[\tilde{\boldsymbol{h}}_{lk}^{H}\boldsymbol{w}_{lj}\right] = M(\beta_{lk} - \gamma_{lk}) \tag{23}$$

where we use the fact that, as a function of $\hat{\boldsymbol{h}}_{lj}$, $\boldsymbol{w}_{lj}$ is independent of $\tilde{\boldsymbol{h}}_{lk}$ for any j and k and $\mathbb{E}\left[\boldsymbol{w}_{lj}\boldsymbol{w}_{lj}^{H}\right] = \boldsymbol{I}_M$ since the precoder is normalized to unit energy by definition. Therefore, from equation (18), the SINR is given by equation (24) and the theoretical spectral efficiency is given by Proposition 1. In FZF, it can be seen that the interference comes from two sources : the first term is the sum of precoding uncertainties of all users and on all subcarriers, and the second term is the ICI depending on the coherent precoding gain on all interfereing subcarriers.

IV. Numerical results

The system described and analyzed in the previous sections is simulated with the following settings inspired from 5G NR RedCap specifications for operation in an indoor scenario [8], [13]. Transmission takes place in a room of size 20×10 meters, considering $L = 4$ APs equipped with $M = 4$ antennas serving $K = 2$ UEs, on a bandwidth $B = 100$ MHz divided in $N = 834$ subcarriers spaced by $\Delta_f = 120$ kHz and at center frequency $f_c = 26$ GHz. The power constraint per AP

$$SINR_k^{\mathrm{MRT}}[\nu] = \frac{M\left|\sum_{l=1}^{L}\psi_{lk}[0]\sqrt{p_{lk}\gamma_{lk}}\right|^2}{\sigma^2+\sum_{j=1}^{K}\sum_{\mu=0}^{N-1}\sum_{l=1}^{L}\left|\psi_{lk}[\nu-\mu]\right|^2 p_{lj}\beta_{lk}+\sum_{\mu\neq\nu}M\left|\sum_{l=1}^{L}\psi_{lk}[\nu-\mu]\sqrt{p_{lk}\gamma_{lk}}\right|^2} \tag{20}$$

$$SINR_k^{\mathrm{FZF}}[\nu] = \frac{(M-K)\left|\sum_{l=1}^{L}\psi_{lk}[0]\sqrt{p_{lk}\gamma_{lk}}\right|^2}{\sigma^2+M\sum_{j=1}^{K}\sum_{\mu=0}^{N-1}\sum_{l=1}^{L}\left|\psi_{lk}[\nu-\mu]\right|^2 p_{lj}(\beta_{lk}-\gamma_{lk})+(M-K)\sum_{\mu\neq\nu}\left|\sum_{l=1}^{L}\psi_{lk}[\nu-\mu]\sqrt{p_{lk}\gamma_{lk}}\right|^2} \tag{24}$$

is $P_{tx} = 100$ mW and the noise power on one subcarrier is $\sigma^2 = -174 + 10\log_{10}(\Delta_f) + N_f$ given in dBm, where the noise figure $N_f = 7$ dBm. The path loss between each terminal, given in dB, is following the model given in [13] for NLoS mmW channels *i.e.* $\beta_{lk} = 72 + 29.2\log_{10}(d_{lk}) + Z$, where d_{lk} is the distance between AP l and UE k given in meters and $Z_{lk} \sim \mathcal{N}(0, \sigma_{sh}^2)$ models the shadow fading with $\sigma_{sh}^2 = 8.7$ dB.

Results are shown in Figure 3 under the form of cumulative distribution function (CDF) of rates for the two precoding schemes under different values of the total CFO $\varphi_l + \theta_k$, set as a constant for all l, k, and corresponding to the values in Hz given in the legend. One point on the CDF is obtained for one realizations of the APs and UEs positions in the room, which determines the path-loss. Plain lines are obtained by the closed form expressions of equations (20) and (24) while markers are obtained by Monte Carlo simulations over 500 channels realizations for a fixed position of APs and UEs. It can be observed that for both precoding schemes, the performance is not significantly degraded for CFO under an order of magnitude of $10^{-7} \times f_c$ in Hz. The maximum degradation obtained here for a CFO of 13 kHz seems to have more impact on FZF precoding than for MRT, where the loss in terms of median rate is around 1 bits/s/Hz against ≈0.3 bits/s/Hz respectively. This suggests that FZF is more sensitive than MRT to the CFO-induced ICI, although it gives better overall performance due to its better ability to reject multiuser interference.

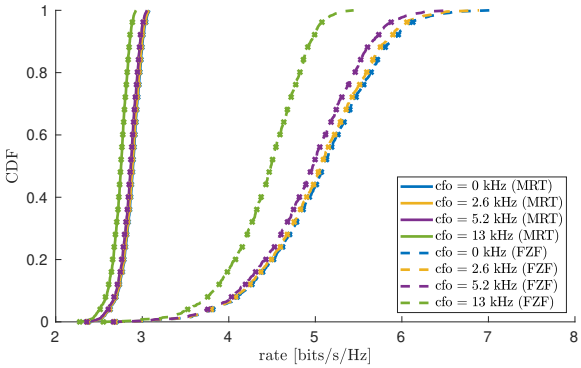

Fig. 3. Rate CDF of MRT and FZF precoding under CFO. Plain and dashed lines are from equations (20) and (24), markers are from Monte Carlo simulations on 500 channels realizations. $L = 4$ APs, $K = 2$ UEs, $M = 4$ antennas per AP, $N = 834$ subcarriers spaced by $\Delta_f = 120$ kHz and $f_c = 26$ GHz (FR2 setting from 5G NR RedCap [8]).

V. Conclusion

In this paper, the DL spectral efficiency of cell-free MIMO OFDM systems is investigated under MRT and FZF precoding scheme and in the presence of CFO. Closed-form expressions are then derived and allow to quantify the effects of such CFO on practical transmissions with imperfect local oscillators. Monte Carlo simulations in an indoor millimeter wave scenario with parameters from 5G RedCap specifications support our results and validate the theoretical expressions given as a function of Rayleigh channels statistics. These results show in particular that MRT on each subcarrier is expected to be more robust against ICI due to CFO.

Further possible extensions of this work include the more general Ricean fading model, as well as the optimal power control towards users and power allocation on the bandwidth.

VI. Acknowledgment

This work has been funded by the French government under the Recovery Plan (CRIIOT project).

Appendix

A. Inter-carrier interference due to CFO at both transmitter and receiver sides, in the noiseless SISO case

Focusing on one subcarrier of a Single Input Single Output (SISO) OFDM system corrupted by CFO at the Tx side, the transmitted symbol can be expressed as the time dependent signal

$$x(t) = \sum_{\nu=0}^{N-1} x[\nu] e^{\,\mathrm{j}2\pi f_\nu t} e^{\,\mathrm{j}2\pi\epsilon_T f_c t} \tag{25}$$

where $f_\nu = \nu\Delta_f = \nu/NT$ and $\epsilon_T f_c = \varphi/NT$ is the transmitter's CFO given in Hz corresponding to the normalized CFO φ.

Considering the channel as time-invariant during one OFDM symbol, the noiseless signal at the input of the receiver is

$$y(t) = \sum_{\nu=0}^{N-1}\sum_{u=0}^{N-1} x[\nu]g(u)e^{\,\mathrm{j}2\pi(f_\nu+\epsilon_T f_c)(t-uT)} \tag{26}$$

where, $g(t) = \sum_{u=0}^{N-1} g(u)\delta(t-uT)$ with $g(u)$ the N samples sequence of the discrete base-band equivalent of $g(t)$, which

eventually vanishes after some index $L < N$ corresponding to the channel length (L should be less than the CP length). The received signal sampled at time $t_n = nT$ becomes:

$$y[n] = \sum_{\nu=0}^{N-1} \sum_{u=0}^{N-1} x[\nu] g(u) e^{\,\mathrm{j}\frac{2\pi}{N}(\nu+\phi)(n-u)} \tag{27}$$

After CP removal, the receiver's DFT processing outputs the projection of the signal onto each tone of the system, so that the observation at the μ^{th} subcarrier can be written as

$$\begin{aligned} y[\mu] = \sum_{\nu=0}^{N-1} \sum_{u=0}^{N-1} x[\nu] g(u) e^{\,-\mathrm{j}\frac{2\pi}{N}(\nu+\varphi)u} \\ \times \frac{1}{N} \sum_{n=0}^{N-1} e^{\,\mathrm{j}\frac{2\pi}{N}(\nu+\varphi-\mu)n} \end{aligned} \tag{28}$$

The ICI term is defined, for $k = 0, \cdots, N-1$, as

$$\begin{aligned} \psi_\varphi[k] &\triangleq \frac{1}{N} \sum_{n=0}^{N-1} e^{\,\mathrm{j}\frac{2\pi}{N}(k+\varphi)n} \\ &= e^{\,\mathrm{j}\pi(k+\varphi)(1-\frac{1}{N})} \frac{\sin\left(\pi(k+\varphi)\right)}{N\sin\left(\frac{\pi}{N}(k+\varphi)\right)} \end{aligned} \tag{29}$$

and let

$$h[\nu;\varphi] = \mathrm{DFT}\left\{ g(n) e^{\,-\mathrm{j}\frac{2\pi}{N}\varphi n} \right\} \tag{30}$$

be the channel frequency response that is actually encountered by the signal taking the CFO into consideration. Thus we have

$$\begin{aligned} y[\mu] &= \sum_{\nu=0}^{N-1} x[\nu] h[\nu;\varphi] e^{\,\mathrm{j}\pi(\nu-\mu+\varphi)(1-\frac{1}{N})} \frac{\sin\left(\pi(\nu-\mu+\varphi)\right)}{N\sin\left(\frac{\pi}{N}(\nu-\mu+\varphi)\right)} \\ &= \sum_{\nu=0}^{N-1} x[\nu] h[\nu;\varphi] \psi_\varphi[\nu-\mu] \end{aligned} \tag{31}$$

Using the same steps considering CFO also at the receiver's side straightforwardly leads to the following instead of (31)

$$y[\mu] = \sum_{\nu=0}^{N-1} x[\nu] h[\nu;\varphi] \psi_{\varphi+\theta}[\nu-\mu] \tag{32}$$

with the same ICI term as in (29), but replacing φ by $\varphi + \theta$.

REFERENCES

[1] Emil Björnson and Luca Sanguinetti, "Scalable cell-free massive mimo systems," *IEEE Transactions on Communications*, vol. 68, no. 7, pp. 4247–4261, 2020.

[2] Giovanni Interdonato, Marcus Karlsson, Emil Björnson, and Erik G. Larsson, "Local partial zero-forcing precoding for cell-free massive mimo," *IEEE Transactions on Wireless Communications*, vol. 19, no. 7, pp. 4758–4774, 2020.

[3] Jiayi Zhang, Jing Zhang, Emil Björnson, and Bo Ai, "Local partial zero-forcing combining for cell-free massive mimo systems," *IEEE Transactions on Communications*, vol. 69, no. 12, pp. 8459–8473, 2021.

[4] Lorenzo Miretti, Emil Björnson, and David Gesbert, "Team mmse precoding with applications to cell-free massive mimo," *IEEE Transactions on Wireless Communications*, vol. 21, no. 8, pp. 6242–6255, 2022.

[5] Özgecan Özdogan, Emil Björnson, and Jiayi Zhang, "Performance of cell-free massive mimo with rician fading and phase shifts," *IEEE Transactions on Wireless Communications*, vol. 18, no. 11, pp. 5299–5315, 2019.

[6] Zahra Mokhtari and Rui Dinis, "Residual cfo effect on uplink sum-rate of cell free massive mimo systems," in *2021 IEEE 94th Vehicular Technology Conference (VTC2021-Fall)*, 2021, pp. 01–06.

[7] Jiakang Zheng, Jiayi Zhang, Emil Björnson, Zhetao Li, and Bo Ai, "Cell-free massive mimo-ofdm for high-speed train communications," *IEEE Journal on Selected Areas in Communications*, vol. 40, no. 10, pp. 2823–2839, 2022.

[8] Sandeep Narayanan Kadan Veedu, Mohammad Mozaffari, Andreas Hoglund, Emre A. Yavuz, Tuomas Tirronen, Johan Bergman, and Y.-P. Eric Wang, "Toward smaller and lower-cost 5g devices with longer battery life: An overview of 3gpp release 17 redcap," *IEEE Communications Standards Magazine*, vol. 6, pp. 84–90, 2022.

[9] Wei Jiang and Hans Dieter Schotten, "Cell-free massive mimo-ofdm transmission over frequency-selective fading channels," *IEEE Communications Letters*, vol. 25, no. 8, pp. 2718–2722, 2021.

[10] T.C.W. Schenk, Xiao-Jiao Tao, P.F.M. Smulders, and E.R. Fledderus, "Influence and suppression of phase noise in multi-antenna ofdm," in *IEEE 60th Vehicular Technology Conference, 2004. VTC2004-Fall. 2004*, 2004, vol. 2, pp. 1443–1447 Vol. 2.

[11] S.M. Kay, *Fundamentals of Statistical Signal Processing: Estimation Theory*, Prentice Hall, 1993.

[12] Emil Björnson, Jakob Hoydis, and Luca Sanguinetti, *Massive MIMO Networks: Spectral, Energy, and Hardware Efficiency*, Foundations and Trends© in Signal Processing, 2017.

[13] Mustafa Riza Akdeniz, Yuanpeng Liu, Shu Sun, Sundeep Rangan, Theodore Ted S. Rappaport, and Elza Erkip, "Millimeter wave channel modeling and cellular capacity evaluation," *IEEE Journal on Selected Areas in Communications*, vol. 32, pp. 1164–1179, 2013.